Coupling Coefficients Between Resonators in Stripline Combline and Pseudocombline Bandpass Filters

Alexander Zakharov and Michael Ilchenko, *Senior Member, IEEE*

***Abstract*— This article discusses the patterns of coupling coefficients between stripline resonators in combline and pseudocombline structures. It was established that there is an electromagnetic (EM) coupling between λ/4 (λ/2) resonators in such structures, and they are bandpass filters (BPFs). Between stripline stepped-impedance resonators (SIRs), both positive and negative mixed couplings can be realized. This coupling can widely vary by changing the shape of resonators and the gap between them. Moreover, the tuning of coupling is carried out without the use of a conducting pin, as in the case of microstrip resonators. The patterns of changes in the coupling coefficients between stripline SIRs at higher resonant frequencies were studied. These changes have a wave-like (alternating) character. The effect of transitioning the coupling coefficient through zero can be used to expand the rejection band of BPF by suppressing the nearest spurious bandwidth. It was found that the coupling coefficients between stripline resonators, all of whose side surfaces are metallized, depend only on the geometric parameters and are not dependent on dielectric constant ε_r. The dielectric constant only moves the coupling frequencies of an insulated stripline structure, while maintaining the ratio between these frequencies. The measurement data for some combline and pseudocombline stripline BPFs are presented.**

***Index Terms*— Combline and pseudocombline coupling structures, discriminating coupling, invariant of coupling coefficient, mixed coupling, rejection band, transmission zero.**

I. Introduction

BANDPASS filters (BPFs) belong to basic components of microwave telecommunication systems [1], [2]. Small-sized filters like filters designed on coaxial dielectric resonators [2], monoblock ceramic filters [3], surface acoustic wave (SAW) filters [4], and multilayer ceramic filters [5], [6] are in great demand. Stripline BPFs, which can overlap a frequency band from 300 MHz to 100 GHz or even higher, show considerable promise [2]. This is due to the possibility of application in these filters of substrates with different values of dielectric constant $\varepsilon_r = 2$–100. The use of thick substrates ($h = 2$–3 mm) allows us to achieve low losses of these BPFs. The use of thin substrates ($h \leq 0.5$ mm) allows us to create thin BPFs with a thickness of 1 mm or less. Stripline BPF can use a wide variety of metallized topological patterns, making it possible to obtain different frequency responses.

Regardless of this advantage, the development of miniature stripline BPFs in recent decades was very limited. In our opinion, this is related to the proposition about the absence of coupling between quarter-wave ($\lambda/4$) or half-wave ($\lambda/2$) stripline resonators placed in parallel to each other or forming a combline or a pseudocombline structure, which was stated in [7]. This statement entered an authoritative publication on contemporary filters [1] and slowed down the process of development of stripline BPFs.

The combline and pseudocombline stripline structures were attributed to the category of unpromising structures. They were even not included in the review of stripline BPFs presented in 1983 [9]. The statement that there is no coupling between $\lambda/4$ or $\lambda/2$ resonators in combline or pseudocombline structures has long been established and requires clarification.

The basis for the design of BPFs is the knowledge of coupling coefficients between resonators and the ability to manage them. The use of mixed coupling coefficients containing magnetic K_m and electric K_e components in BPFs makes their frequency responses more diverse by introducing transmission zeros into them. Such couplings are also called "frequency dependent" [10] or "resonant" [11]. Mixed couplings are implemented in BPFs on various transmission lines, such as coaxial [12], multilayer [13], substrate integrated waveguide [14]–[16], and microstrip [17]–[21]. If a BPF has N tuned mixed couplings between adjacent resonators, then we can have N adjustable transmission zeros at real frequencies. Cited articles differ from each other in ways of implementing mixed coupling coefficients that depend on the transmission line construction, type of resonators used, and their parameters. The mixed coupling between resonators of different transmission line constructions is studied well. At the same time, the mixed couplings between stripline resonators are not well studied.

A large number of articles are devoted to the extension of rejection band of BPF. We will select three of them [22]–[24], which use discriminating couplings between resonators to suppress spurious passbands. In [22], open-loop resonators were used. In [23], two types of resonators $\lambda/4$ and $\lambda/2$ were used simultaneously. In [24], discriminating couplings were realized

Manuscript received December 11, 2019; revised March 12, 2020; accepted March 19, 2020. The work of Alexander Zakharov was supported by the Ministry of Education of Ukraine under Project 0119U100622. *(Corresponding author: Alexander Zakharov.)*

The authors are with the Telecommunication Department of National Technical University of Ukraine "Igor Sikorsky Kyiv Polytechnic Institute," 03056 Kyiv, Ukraine (e-mail: azakharov217@gmail.com).

Color versions of one or more of the figures in this article are available online at http://ieeexplore.ieee.org.

Digital Object Identifier 10.1109/TMTT.2020.2988866

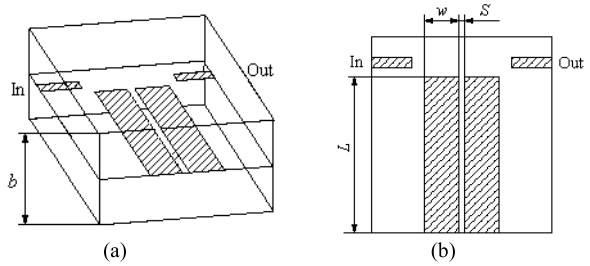

Fig. 1. Stripline quarter-wave resonator. (a) 3-D view. (b) Topology.

between stepped-impedance resonators (SIRs) of two different types, quarter wave and half wave. In these articles, microstrip BPFs were considered. It is also advisable to explore the possibility of implementing discriminating couplings between stripline resonators.

This article explores the coupling coefficients between resonators in combline and pseudocombline stripline BPFs. The article is organized as follows. Section II analyzes coupling coefficients between stripline $\lambda/4$ resonators. Section III analyzes mixed couplings between stripline quarter-wave SIRs. Design of small-sized quasi-elliptic BPF with high dielectric constant $\varepsilon_r = 92$ is performed. Section IV analyses coupling coefficients between stripline SIRs of quarter-wave type at higher resonance frequencies. The design of the thin (1 mm) BPF with wide rejection band, achieved due to the zero coupling coefficient at the frequency of the parasitic resonance, is performed. Section V considers a new property of electromagnetic (EM) interaction between resonators in closed stripline structures. Our conclusion is given in Section VI.

II. Stripline Quarter-Wave Resonators

Let us consider a pair of stripline quarter-wave resonators (Fig. 1). The stripline design is filled with dielectric having dielectric constant ε_r, and its thickness is equal to b. Central conductors of these resonators are characterized by width w and length L. They are separated by the gap S. The bottom and top of the base and the sides of the structure are metallized, which makes it insulated. One end of the central conductors is open and the other one is short circuited to the conductive wall.

A. Coupling Coefficient Between λ/4 Resonators

Each stripline resonator has many resonance frequencies, and the lowest of which f_0 is the main one. At frequency f_0, the resonator in question is a quarter-wave resonator. Let us consider the EM interaction of the pair of resonators at the main resonance frequency that is characterized by the coupling coefficient K. The values of K can be calculated by the following formula [8]:

$$k = \frac{f_o^2 - f_e^2}{f_o^2 + f_e^2} \tag{1}$$

where f_e and f_o are the frequencies of even and odd modes of oscillations, respectively. The insertion loss response of a pair of stripline resonators weakly coupled with input and output loads contains two pronounced peaks corresponding to the

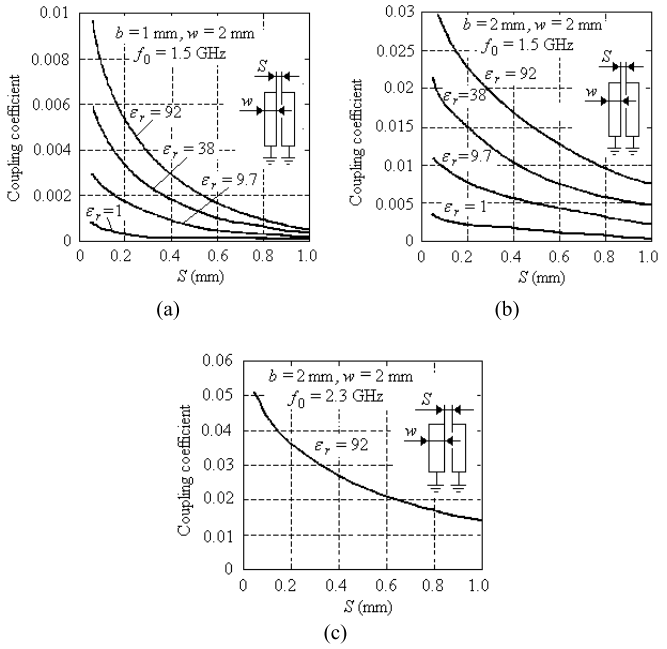

Fig. 2. Coupling coefficient between stripline $\lambda/4$ resonators with width $w = 2$ mm. (a) For $f_0 = 1.5$ GHz, $b = 1$ mm. (b) For $f_0 = 1.5$ GHz, $b = 2$ mm. (c) For $f_0 = 2.3$ GHz, $b = 2$ mm and $\varepsilon_r = 92$.

coupling frequencies. The simulation of frequency responses involved the use of commercial program Microwave Office (AWR Company). Excitation of resonators was performed through capacitive gaps.

Fig. 2(a) illustrates the effect of gap S and dielectric constant ε_r on coupling coefficient K at the thickness of stripline structure $b = 1$ mm. The simulation was performed by assuming the following values: $\varepsilon_r = 92$, 38, 9.7, and 1; $w = 2$ mm; and the value of gap S was varied from 0.05 to 1 mm. At $\varepsilon_r = 92$, the length of resonator was assumed to be equal to $L = 5$ mm, and its corresponding resonance frequency $f_0 \approx 1508$ MHz. At other values of ε_r, the lengths of resonators were selected in such way that their resonance frequencies would coincide with the previous value of f_0: at $\varepsilon_r = 38$, $L = 7.9$ mm; at $\varepsilon_r = 9.7$, $L = 15.8$ mm; and at $\varepsilon_r = 1$, $L = 49.5$ mm. The dependencies in Fig. 2(a) show that the more the ε_r is, the more is the K.

Fig. 2(b) presents the relationship of K as a function of gap S and dielectric constant ε_r at doubled thickness of stripline $b = 2$ mm. In this case, the values of K increased more than three times, which indicates that the increase in the thickness of b leads to an increase in K.

Fig. 2(c) presents the K–S relationship for a pair of stripline resonators with $\varepsilon_r = 92$, $b = 2$ mm, $w = 2$ mm, and the length of which is reduced to $L = 3$ mm. These resonators have a higher resonance frequency $f_0 \approx 2.3$ GHz. Comparison of dependences in Fig. 2(b) and (c) shows that the increase in the resonant frequency of resonators f_0 leads to the growth of K. Data in Fig. 2(a)–(c) allow us to formulate the patterns of the variation of coupling coefficient K for stripline quarter-wave resonators in combline structure. To increase the K result, increase ε_r, increase the thickness of stripline b, and increase the resonance frequency f_0.

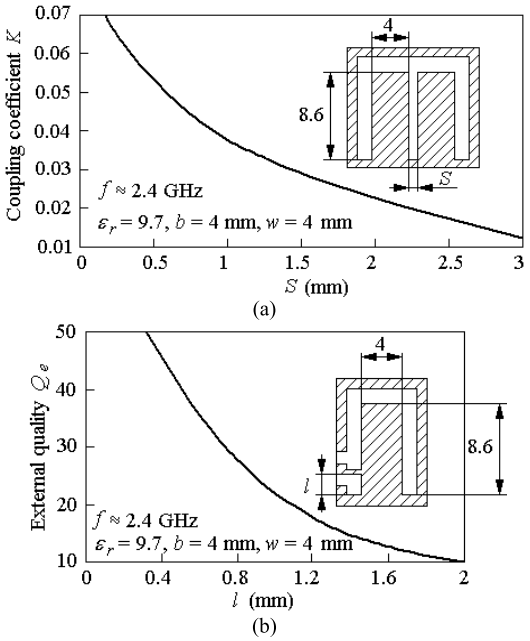

Fig. 3. Dependencies used in the design of the stripline BPF. (a) Coupling coefficient. (b) External quality factor.

B. Stripline Combline BPF

Let us design a fourth-order stripline combline BPF with Chebyshev response corresponding to the following requirements: center frequency $f_0 = 2380$ MHz; fractional bandwidth FBW $= 0.035$; and passband ripple $L_{\mathrm{Ar}} = 0.1$ dB. Using the initial data and parameters of Chebyshev low-pass prototype $g_0, g_1, \ldots, g_n, g_{n+1}$ corresponding to the specified values of n and L_{Ar} and using the known formulas [1]

$$K_{i,i+1} = \frac{\mathrm{FBW}}{\sqrt{g_i g_{i+1}}} \quad \text{for } i = 1, \ldots, n-1 \tag{2}$$

$$Q_{e1} = \frac{g_0 g_1}{\mathrm{FBW}}, \quad Q_{e2} = \frac{g_n g_{n+1}}{\mathrm{FBW}}. \tag{3}$$

We can determine the coupling coefficients between adjacent resonators $K_{i,i+1}$ and external Q-factors, Q_{e1} and Q_{e2} of end resonators. For $L_{\mathrm{Ar}} = 0.1$ dB and $n = 4$, using tables [1], we can find g-parameters: $g_0 = 1$, $g_1 = 1.1088$, $g_2 = 1.3062$, $g_3 = 1.7704$, $g_4 = 0.8181$, and $g_5 = 1.3554$. Substituting these values of g-parameters and the initial data into (2) and (3), we obtain $K_{12} = K_{34} = 0.029$; $K_{23} = 0.023$; and $Q_e = 31.7$.

The design of the filter is formed by connecting two dielectric substrates from alumina having thickness $h = 2$ mm, $\varepsilon_r = 9.7$, and $\tan\delta = 0.0002$. The filters are fully shielded because all of their side surfaces are metallized.

Fig. 3 shows the dependencies used in the design, and the insets show filter elements. The central conductors of these resonators are characterized by width $w = 4$ mm. The short-circuited ends of the resonators are connected to a "protective" band of 1-mm width, which prevents tin from getting inside the filter during its assembly. The length of resonators, counted from this strip, is equal to $L = 8.6$ mm. The resonators are separated by the gap S. The "protective" strip leads to a slight increase in coupling coefficients.

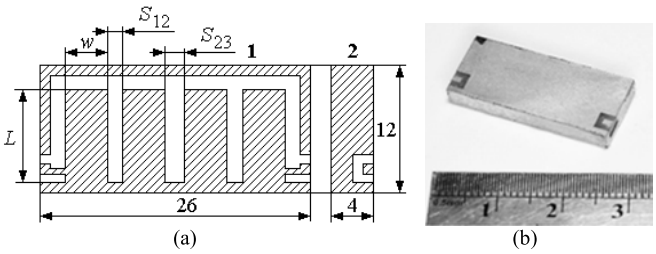

Fig. 4. Stripline combline BPF. (a) Topology. (b) Photograph of the fabricated filter.

Fig. 3(a) presents the relationship $K = K(S)$ for stripline resonators. According to this curve, we determine that the coupling coefficients $K_{12} = K_{34} = 0,029$ and $K_{23} = 0.023$ correspond to the gaps $S_{12} = S_{34} = 1.5$ mm and $S_{23} = 2.0$ mm.

As shown in the inset to Fig. 3(b), circuit ensures the coupling of end resonator with load 50 Ω. It represents a segment of stepped-impedance stripline with a width of 1 and 0.5 mm. This segment is removed from the "protective" band by distance l. The value of external Q-factor of end resonator Q_e is adjusted by distance l. The values of external Q-factor Q_e can be expediently determined by using the results of the EM simulation of group delay of parameter S_{11} for resonator with one-sided load [8]. The Q_e can be calculated by using the following expression:

$$Q_e = \frac{\pi f_0 \tau_{S_{11}}(f_0)}{2} \tag{4}$$

where $\tau_{S_{11}}(f_0)$ is the group delay at the resonance frequency f_0. Fig. 3(b) presents the relationship $Q_e = Q_e(l)$ based on (4). The value of external Q-factor $Q_e = 31.7$ is obtained at $l = 0.7$ mm.

Dielectric substrates with alumina were coated with a layer of copper of 8 μm in thickness using vacuum deposition. The topology of central conductors of the filter is shown in Fig. 4(a) (position *1*), where dimensions are specified in millimeters. The size of the filter is 26 mm × 12 mm × 4 mm. When assembling a filter, substrates with conductive layers are pressed to each other according to the "face-to-face" principle and their metallized ends are soldered together. Conductive strips on the two ends of the filter, which are shown in Fig. 4(a) (position 2), connect the inner and outer parts of the filter. The latter ones are contact pads. They are shown in the filter photograph presented in Fig. 4(b), where the filter is shown on the reverse side. The filter design is intended for surface mounting.

Frequency responses of the stripline BPF are presented in Fig. 5. The measured filter characteristics are center frequency $f_0 = 2380$ MHz, bandwidth BW $= 85$ MHz, insertion loss at the center frequency $IL_0 = 1.3$ dB, return loss $RL \leq$ –13.0 dB, and selectivity 40 dB ($f_0 \pm 115$ MHz).

Thus, there is EM coupling between the stripline combline ($\lambda/4$) resonators, and the stripline combline structure is BPF.

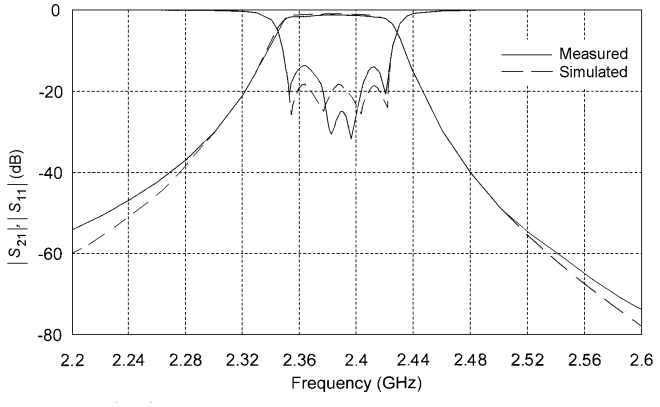

Fig. 5. Frequency responses of stripline combline BPF.

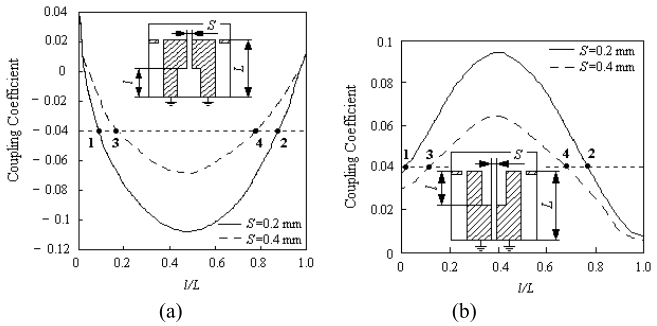

Fig. 6. Coupling coefficient between stripline SIRs. (a) Short-circuited end of SIR is narrow. (b) Open end of SIR is narrow.

III. Mixed Couplings Between Stripline Resonators

The mixed coupling coefficient K has magnetic K_m and electric K_e components [8]

$$K = K_m + K_e. \tag{5}$$

The "+" sign is assigned to the magnetic component and the "–" sign is assigned to the electrical one. In second-order BPF with mixed coupling, an f_z transmission zero is generated, the position of which is expressed by the well-known formula [12], [18]

$$f_z = f_0\sqrt{\mathrm{K_m}/|K_e|}. \tag{6}$$

A transmission zero may be above or below f_0. If $K > 0$, then $f_z > f_0$, and if $K < 0$, then $f_z < f_0$. The pattern (6) allows us to move the transmission zero f_z with respect to f_0 for a fixed value of $|K|$. If the BPF contains N mixed couplings, it can have N transmission zeros.

The design principle of a BPF with mixed couplings between adjacent resonators is as follows. Using expression (2), the absolute values $|K|$ of mixed coupling coefficients are determined. Each coupling coefficient is associated with a predetermined transmission zero f_z. Based on (5) and (6), the components K_m and K_e of each mixed coupling coefficient are determined. It is reasonable to study the mixed coupling between stripline SIRs for implementing BPF with predefined transmission zeros.

A. Electromagnetic Interaction Between Stripline SIRs

Fig. 6 shows the dependence of K on the form of closely placed stripline SIRs, one end of which is short circuited. These dependences are constructed for two characteristic shapes of the resonators, which are shown in the insets. The following parameters of SIR were used: the thickness $b = 2$ mm; the dielectric constant $\varepsilon_r = 92$; the resonator length $L = 3.6$ mm; the width of the wide part of the SIR $w_1 = 1.4$ mm; and narrow width of the SIR $w_2 = 0.9$ mm. The length l of the narrow section of the resonator is variable. The solid lines correspond to the gap 0.2 mm between the resonators and dashed lines correspond to the gap 0.4 mm. For the pair of resonators shown in Fig. 6(a), the values of K can be positive, negative, and equal to zero. For positive mixed coupling coefficient ($K > 0$), the magnetic component K_m dominates in it. For $K < 0$, the electrical component dominates. With increasing length l of a narrow part of the resonator [Fig. 6(a)], the value of K decreases to zero firstly. Then it becomes negative and increases in absolute value. The value of $K < 0$ for almost all values of l is changed. The functions $K = K(l/L)$ are bell shaped and they have a minimum at $l/L \approx 1/2$. The largest change in K occurs when the gap between the resonators is equal to 0.2 mm: $-0.106 \le K \le 0.0385$.

For the pair of resonators shown in Fig. 6(b), the values of K are always positive. The curves of $K = K(l/L)$ are bell shaped. They have the maximum at $l/L \approx 1/2$. When the gap between the resonators is 0.2 mm, the values of K vary within $0.0385 \le K \le 0.0948$. In the two cases considered, the mixed coupling coefficient between stripline SIRs changed in a wide enough range $-0.106 \le K \le 0.0948$. Note that the change in K over a wide range is carried out without the use of an additional conductive pin between two resonators, as in the case of microstrip SIRs [19].

The dependences $K(l/L)$, similar to shown in Fig. 6(a), can also be obtained if the narrow part of the SIR is located near the open end but in its "inner" part. The dependences $K(l/L)$, similar to shown in Fig. 6(b), can also be obtained if the narrow part of the SIR is located near the short-circuited end but in its "internal" part.

Fig. 7 shows symmetric fourth-order BPFs with alternating signs of mixed coupling coefficients that have two both sided transmission zeros. Filters in Fig. 7(a) and (b) have two couplings with $K < 0$ and one coupling with $K > 0$. The filters in Fig. 7(c) and (d) have two positive mixed couplings and one negative mixed coupling.

The coupling coefficients K in Fig. 6(a) and (b) are mixed. Expressions (5) and (6) allow us to determine the components of K_m and K_e if the values of K and f_z are known. The center frequency f_0 in (6) is defined as follows: $f_0 = (f_o + f_e)/2$. Table I shows the values of K_m and K_e for four points in Fig. 6(a) with the same negative mixed coupling coefficient $K = -0.04$. Each curve in Fig. 6(a) intersects line $K = -0.04$ at two points. Points 1 and 2 correspond to the gap $S = 0.2$ mm between resonators. Points 3 and 4 correspond to the gap $S = 0.4$ mm. Fig. 8(a) shows the SIR topologies corresponding to these points.

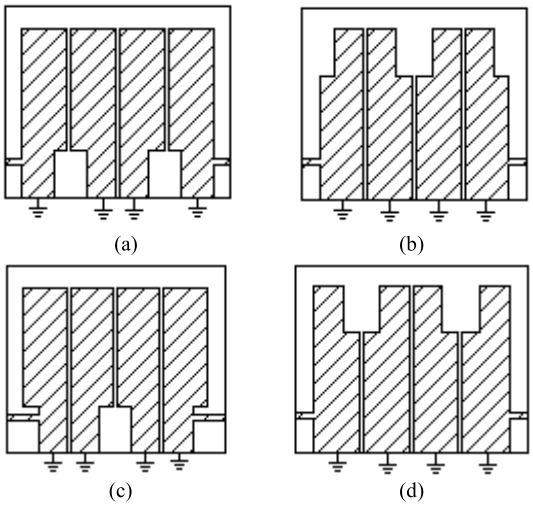

Fig. 7. Fourth-order stripline BPFs with alternating mixed couplings. (a) Two negative and one positive couplings, short-circuited end of SIR is narrow. (b) Two negative and one positive couplings, open-circuited end of SIR is narrow. (c) Two positive and one negative couplings, short-circuited end of SIR is narrow. (d) Two positive and one negative couplings, open-circuited end of SIR is narrow.

TABLE I
COMPONENTS OF MIXED COUPLING $K = -0.04$ AT POINTS 1, 2, 3, AND 4 IN FIG. 6(A)

No.	1	2	3	4
l/L	0.0903	0.8819	0.1806	0.7917
K_m	0.1295	0.0642	0.0658	0.0479
K_e	− 0.1695	− 0.1042	− 0.1058	− 0.0879
$K_m/\lvert K_e\rvert$	0.764	0.616	0.622	0.545

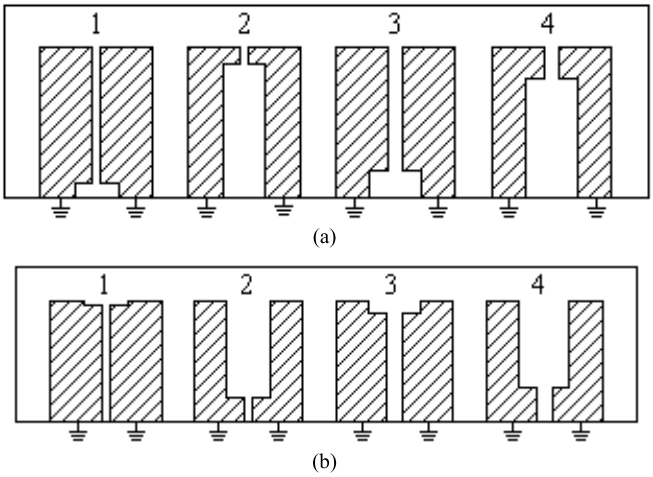

Fig. 8. Pairs of SIRs with mixed coupling coefficient $|K| = 0.04$. (a) Pairs of SIRs corresponding to points 1, 2, 3, and 4 in Fig. 6(a) for $K = -0.04$. (b) Pairs of SIRs corresponding to points 1, 2, 3, and 4 in Fig. 6(b) for $K = 0.04$.

Table II presents the values of K_m and K_e for four points in Fig. 6(b) with the same positive mixed coupling coefficient $K = 0.04$. As in the previous case, points 1 and 2 correspond to the gap $S = 0.2$ mm between two resonators. Points 3 and 4 correspond to the gap $S = 0.4$ mm. Fig. 8(b) shows the SIR topologies corresponding to these points.

TABLE II
COMPONENTS OF MIXED COUPLING $K = -0.04$ AT POINTS 1, 2, 3, AND 4 IN FIG. 6(B)

No.	1	2	3	4
l/L	0.0139	0.7917	0.0972	0.7917
K_m	0.2305	0.0829	0.1559	0.0699
K_e	− 0.1905	− 0.0429	− 0.1159	− 0.0299
$K_m/\lvert K_e\rvert$	1.210	1.932	1.345	2.338

The data presented in Tables I and II and Fig. 8 indicate that the mixed coupling coefficient K can be implemented on a set of SIRs of various shapes and with different gaps between resonators. The differences between these pairs of resonators lie in the values of the components K_m and K_e and, therefore, in the position of the transmission zero f_z relative to f_0. The shape of the resonators and the gap between them allow us to adjust the position of f_z relative to f_0.

Analysis shows the following patterns.

1) The convergence of stripline SIRs, i.e., decreasing the gap S between them leads to an increase in the components K_m and K_e for a fixed value of K. In this case, the ratio $K_m/|K_e|$ approaches unity and interval between frequencies f_z and f_0 decreases.
2) For a fixed gap S between stripline SIRs, a smaller ratio of lengths l/L leads to a smaller interval between frequencies f_z and f_0.
3) The degree of convergence of the frequencies f_z and f_0 is limited by the minimum allowable gap S between stripline resonators.
4) Two mixed coupling coefficients K_1 and K_2 are equal to each other if $K_{1\,m} = K_{2\,m}$ and $K_{1\,e} = K_{2\,e}$. The mixed coupling coefficients at points 1, 2, 3, and 4 (Fig. 6) do not satisfy these conditions.

B. Small-Sized Stripline Quasi-Elliptic BPF

We realize a fourth-order stripline combline filter. This filter has a Chebyshev characteristic in the passband and following specification:

Center frequency: $f_0 = 1835$ MHz
Bandwidth: BW = 90 MHz (FBW = 0.049)
Return loss: $RL < -13.5$ dB
Transmission zeros: f_{z1}, $f_{z2} \in [f_0 \pm 200$ MHz].

In this case, two transmission zeros are not defined exactly. They should be removed from f_0 no more than 200 MHz providing increased frequency selectivity. The specified value of return loss $RL = -13.5$ dB corresponds to the ripple value: $L_{\mathrm{Ar}} \approx 0.2$ dB. For designing the filter with the values $L_{\mathrm{Ar}} \approx 0.2$ dB and $n = 4$, the next g-parameters are used [1]: $g_0 = 1$, $g_1 = 1.3028$, $g_2 = 1.2844$, $g_3 = 1.9761$, $g_4 = 0.8468$, and $g_5 = 1.5386$. Substituting these values and the value FBW = 0.049 into (2) and (3), we obtain $|K_{12}| = |K_{34}| = 0.0379$, $|K_{23}| = 0.0308$, and $Q_e = 26.59$. We take the values of K_{12} and K_{34} positive and $K_{23} < 0$.

These coupling coefficients are mixed and their components K_m and K_e must provide the required location of the transmission zeros. The transmission zero for the positive K_{12} value

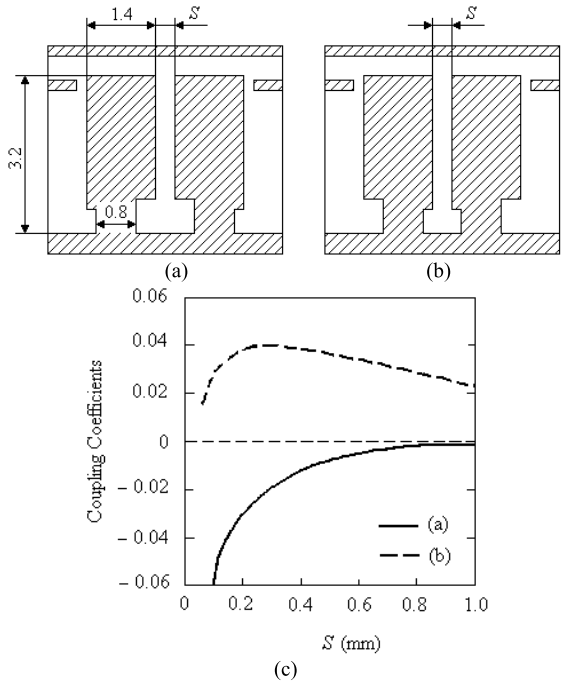

Fig. 9. Resonator pairs of the developed BPF with mixed coupling coefficients. (a) Pairs of SIRs with $K < 0$. (b) Pairs of SIRs with $K > 0$. (c) Dependence of the value K on the gap S.

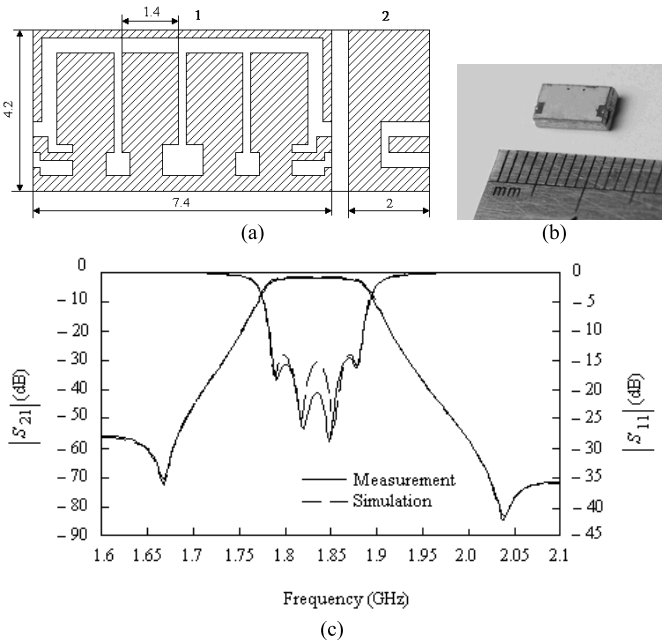

Fig. 10. Miniaturized quazi-elliptic stripline BPF with mixed couplings. (a) Topology. (b) Photograph of the fabricated filter. (c) Frequency responses.

is denoted by f_{z1}. According to the accepted specification, we have $f_{z1} \leq f_0 + 200$ MHz. From this inequality, we define $f_{z1}/f_0 \leq 1.109$. Using (6), we write the condition that the components K_{m12} and K_{e12} must satisfy

$$K_{m12}/|K_{e12}| \leq 1.23. \tag{7}$$

The transmission zero for a negative K_{23} value is denoted as f_{z2}. According to the accepted specification, we have $f_{z2} \geq f_0 - 200$ MHz, hence, it follows $f_{z2}/f_0 \geq 0.891$. Using (6), we finally get the following:

$$K_{m23}/|K_{e23}| \geq 0.794. \tag{8}$$

In the developed stripline BPF, two thermostable dielectric substrates with $\varepsilon_r = 92$ and $\tan\delta = 0.0003$ are used. The thickness of the substrates is $h = 1$ mm and thickness of the stripline filter is $b = 2$ mm.

Fig. 9(a) and (b) shows the topology of the resonator pairs of the developed filter. Both pairs contain the same resonators, which are oriented relative to each other in different ways. As a result, the pair of resonators in Fig. 9(a) is characterized by the value $K < 0$ and the pair of resonators in Fig. 9(b) is characterized by the value $K > 0$.

The short-circuited ends of the resonators are connected to a "protective" strip of 0.4-mm width. The length of each resonator, counted from this strip, is equal to $L = 3.2$ mm and the maximum width of the resonator is $w = 1.4$ mm. In the area of the short circuit, two rectangles of 0.8 mm $\times$ 0.4 mm and 0.6 mm $\times$ 0.2 mm were extracted from the central strip of the resonator. As a result, the resonator becomes step-impedance and tuned to the frequency f_0. The protective strip in the short-circuit end region of the resonators increases the magnetic component K_m of the mixed coupling. The wider it is, the more the K_m is. This led to the fact that in pair of resonators [Fig. 9(b)] with $K > 0$, the width of the conductors was reduced in the area of the short circuit ends.

Using computer simulation, we present the dependences $K = K(S)$ in Fig. 9(c) for the considered pairs of resonators. Values $K_{12} = K_{34} = 0.0379$ are realized on a pair of resonators shown in Fig. 9(b) at $S_{12} = S_{34} = 0.2$ mm. The value of $K_{23} = -0.0308$ is implemented on a pair of resonators shown in Fig. 9(a) at $S_{23} = 0.2$ mm. Using (5) and (6), we determine the components of K_{m12} and K_{e12} of the mixed coupling K_{12}: $K_{m12} = 0.2079$ and $K_{e12} = -0.170$. These components satisfy the condition (7), which is derived from the specification. Similarly, we determine the components K_{m23} and K_{e23} of the mixed coupling K_{23}:$K_{m23} = 0.1547$ and $K_{e23} = -0.1855$. These components satisfy the condition (8).

Combining the pairs of resonators shown in Fig. 9 leads to a fourth-order BPF shown in Fig. 10. Dielectric substrates with $\varepsilon_r = 92$ and $\tan\delta = 0.0003$ were coated with a layer of copper of 8 μm in thickness using vacuum deposition. The topology of the central conductors of the filter is shown in Fig. 10(a) (position 1), where dimensions are indicated in millimeters. The size of the filter is 7.4 mm $\times$ 4.2 mm $\times$ 2 mm. The use of the "protective" strip of 0.4-mm width has resulted in a different topology for this filter from the filter topology shown in Fig. 7(b). Conductive strips on the two ends of the filter, which are shown in Fig. 10(a) (position 2), connect the inner and outer parts of the filter. The latter ones are contact pads. They are shown in the filter photograph presented in Fig. 10(b), where the filter is shown on the reverse side. The required external quality factor of the end resonators $Q_e = 26.59$ is provided by the appropriate choice (4) of the connection coordinates of the I/O strips.

The measured and simulated frequency responses of the filter are shown in Fig. 10(c). The measured filter characteristics

are center frequency $f_0 = 1835$ MHz, BW $= 90$ MHz, insertion loss at the center frequency $IL_0 = 1.9$ dB, insertion loss at the edges of the passband $IL_{\max} = 3.2$ dB, and return loss $RL \leq -14.0$ dB.

Two transmission zeros of the filter are located at frequencies $f_{z1} = 2034$ MHz and $f_{z2} = 1668$ MHz, which correspond to the previously accepted specification. The filter has an increased selectivity of 45 dB ($f_0 \pm 135$ MHz). When using a normalized frequency $j\Omega = (f/f_0 - f_0/f)/\text{FBW}$, the selectivity can be presented in the form of 45 dB ($\pm j3$). For comparison, we note that the fourth-order "High-Perf Ceramic Monoblock Filter CER0206A" [25] with dimensions 7.1 mm × 5.6 mm × 4 mm, $f_0 = 1880$, and BW $= 60$ MHz has lower selectivity: 42 dB($-j3.3$) and 24 dB($j3.3$).

Extremely important is the effect of the transition of the mixed coupling coefficient through the zero value, as shown in Fig. 6(a). In this moment, the components of the mixed coupling are equal to each other $K_m = |K_e|$. If a hairpin resonator is placed over a pair of such resonators and open ends of this hairpin resonator are turned in the direction of the first two resonators, a third-order BPF is formed. The mixed coupling of the formed filter is cross-coupling one. Such a filter has a quasi-elliptic frequency response with two transmission zeros located equidistant relative to f_0 [20]. The larger the value of $K_m = |K_e|$, the closer the transmission zeros to f_0. If the hairpin resonator is replaced with a quarter-wave resonator, then the newly formed filter will have a flat group delay [21]. These effects were demonstrated in [20] and [21] for microstrip BPFs. However, they can also be used in stripline BPFs that are self-shielded, and their resonators have a higher unloaded quality factor Q_u than microstrip resonators. The transition of the mixed cross-coupling coefficient through the zero value gives the third-order filter, the properties that are inherent in a quadruplet BPF with all simple couplings.

The use of substrates with a low dielectric constant ($\varepsilon_r = 2.2$) allows the filters in question to operate at frequencies of 100 GHz and higher, which is consistent with the results given in [2].

IV. Coupling Coefficients at Higher Resonant Frequencies

Fig. 11(a) and (b) shows two types of low-profile ($b = 1$ mm) stripline SIRs with dielectric constant $\varepsilon_r = 9.7$ (alumina), whose length is $L = 10$ mm. The maximum width of the resonator is 1.6 mm ($Z_{0\min} = 14.75\ \Omega$), and the minimum width of the resonator is 0.8 mm ($Z_{0\max} = 24.26\ \Omega$). The resonators are separated by the gap $S = 0.1$ mm.

A. Coupling Coefficients Vs Shape of SIRs

These resonators are characterized by many oscillations with resonant frequencies f_n, $n = 0, 1, \ldots$, which are electromagnetically coupled to each other. Let us denote K_0, K_1, and K_2 coupling coefficients corresponding to resonance frequencies f_0, f_1, and f_2. Fig. 11(c) and (d) shows the dependences of K_0, K_1, and K_2 on the normalized value l/L of these SIRs.

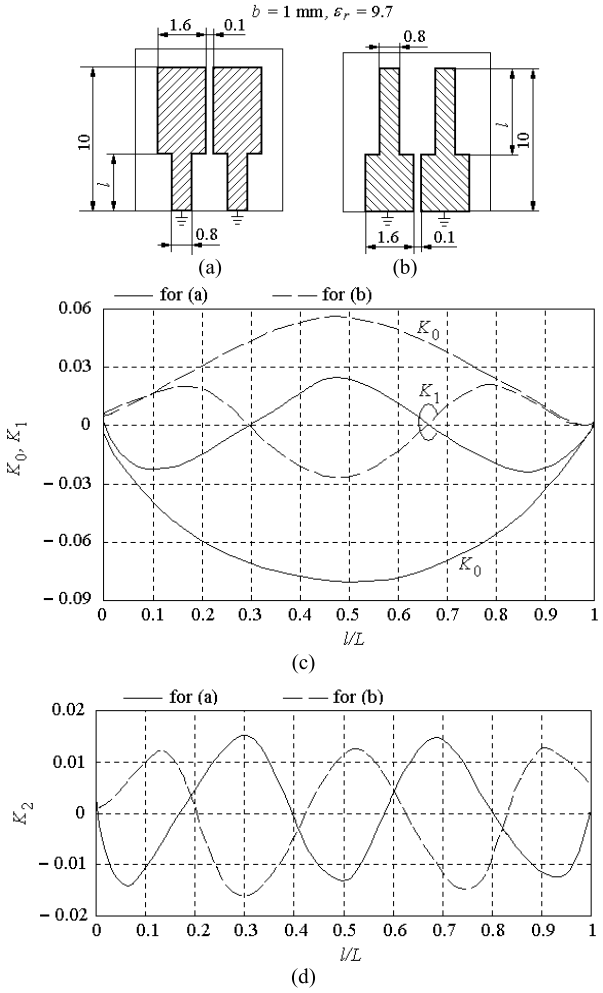

Fig. 11. Coupling coefficients between low-profile stripline SIRs. (a) First-type SIRs. (b) Second-type SIRs. (c) Coupling coefficients K_0 and K_1. (d) Coupling coefficients K_2.

Let us mention the characteristic features of curves $K_n = K_n(l/L)$ shown in Fig. 11(c) and (d),

1) Functions $K_n(l/L)$ demonstrate alternating behavior; the number of extremes of these curves is $2n + 1$.
2) The number of internal zeros of function $K_n(l/L)$ is $2n$. The coupling coefficients K_0, K_1, and K_2 are mixed. Condition for suppression of the first spurious passband $K_1 = 0$ is of the greatest interest, because, in this case, the rejection band of the BPF expands.

Plots in Fig. 11(c) show that the condition $K_1 = 0$ holds for $l/L \approx 1/3$ and $l/L \approx 2/3$ for both types of resonator pairs. To determine which pair of resonators in Fig. 11(a) and (b) gives preference, additional analysis is necessary.

Resonance frequencies of considered SIRs [Fig. 11(a) and (b)] can be determined from the resonance equations

$$m \tan[\omega(L-l)/v] = -\cot(\omega l/v) \quad \text{for the first type;} \quad (9')$$

$$m^{-1} \tan[(\omega l/v)] = -\cot[\omega(L-l)/v] \quad \text{for the second type} \quad (9'')$$

where v is the propagation speed of EM wave, and $m = Z_{0\max}/Z_{0\min}$. Fig. 12 shows the plots of the ratio of resonance frequencies f_2/f_0, which characterize the distance

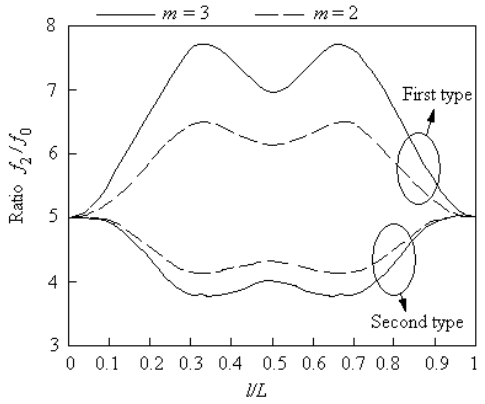

Fig. 12. Ratio f_2/f_0 of stripline SIRs.

between these frequencies. These curves show that the SIR of the first type is more preferable because it has higher value f_2/f_0. For a pair of resonators of the first type, upper curves f_2/f_0 (Fig. 12) have two maximum at $l/L = 1/3$ and at $l/L = 2/3$. It follows from expression (9′) that, for the SIR, the ratio f_2/f_0 is given by the formula

$$\frac{f_2}{f_0} = \frac{\pi}{\tan^{-1}\sqrt{1/(1+2m)}} - 1 \tag{10}$$

from which we find that $f_2/f_0 = 6.47$ for $m = 2$ and $f_2/f_0 = 7.69$ for $m = 3$.

Comparison of the curves in Figs. 11(c) and 12 shows that there is a double effect at points $l/L \approx 1/3$ and $l/L \approx 2/3$: the zero value of $K_1 = 0$ and the maximum ratio f_2/f_0. Combining both effects, we can obtain a significant expansion of the BPF rejection band.

B. Low-Profile Stripline BPF With Extended Stopband

To demonstrate the described above effect ($K_1 = 0$), a third-order Chebyshev filter centered at $f_0 = 2.45$ GHz, with a 0.2-dB bandpass ripple and BW = 140 MHz (FBW = 0.057), was designed. According to [1], these values give the coupling coefficients $K_{12} = K_{23} = K_0 = 0.048$ and external quality factor of end resonators $Q_e = 21.5$. The low-profile ($b = 1$ mm) stripline BPF with SIRs was fabricated from the alumina substrates with thickness $h = 0.5$ mm. Topology of the filter is depicted in Fig. 13(a), position 1. Some dimensions are in millimeters: $l = 2.1$ mm, $L = 7.8$ mm ($l/L = 0.27$), $w_{\max} = 1.6$ mm ($Z_{0\min} = 14.75\ \Omega$), $w_{\min} = 0.8$ mm ($Z_{0\max} = 24.26\ \Omega$), $S = 0.2$ mm, $t = 1.2$ mm, and BPF size is 9 mm × 7.6 mm × 1 mm. Conducting segments were formed on the BPF faces [Fig. 13(a), position 2]. These segments connect internal and external filter parts. The external part is depicted in the filter photograph presented in Fig. 13(b), where the filter is shown on the reverse side.

Fig. 14(a) plots coupling coefficients K_0 and K_1 with various gap values S. If $S = 0.2$ mm, then $|K_0| = 0.048$. Although the resonators in the inset to Fig. 14(a) are not identical as in Fig. 11(a), the coupling coefficient $K_1 = 0.0032$ is quite small for given parameters. Fig. 14(b) plots external quality factor Q_e with different t values. If $t = 1.2$ mm, then $Q_e = 21.5$.

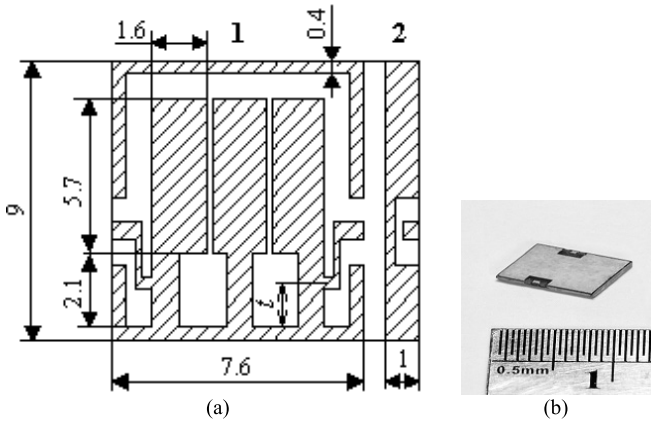

(a) (b)

Fig. 13. Low-profile stripline BPF with $K_1 = 0$. (a) Topology. (b) Photograph of the fabricated filter.

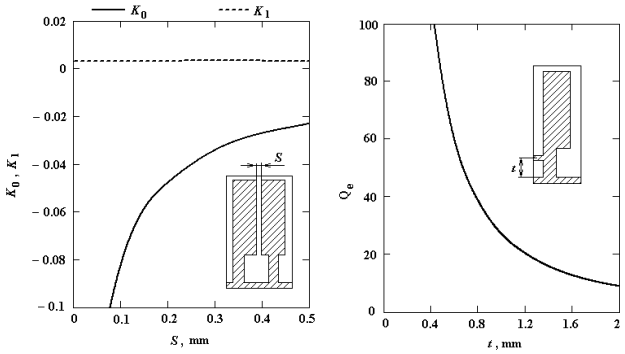

(a) (b)

Fig. 14. Design plots for low-profile stripline BPF. (a) Coupling coefficients K_0 and K_1. (b) External quality factor Q_e.

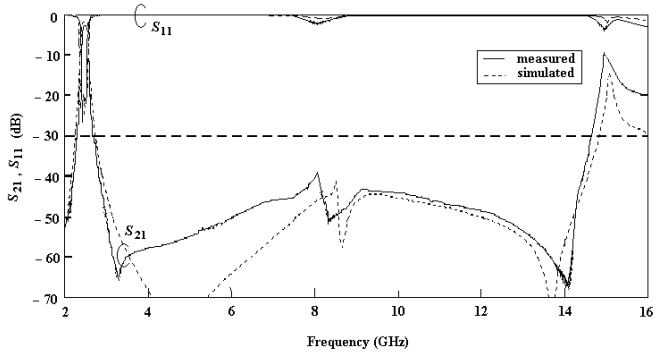

Fig. 15. Measured and simulated frequency responses of low-profile stripline BPF with $K_1 = 0$.

The measured and simulated frequency responses of the filter are shown in Fig. 15. The measured data are $f_0 = 2450$ MHz; BW = 140 MHz; $IL_0 = 1.8$ dB; and $RL < -16$ dB. Spurious bandpass associated with resonant frequency f_1 is suppressed as predicted. First spurious bandpass of the BPF is 6.06 f_0. SIRs of the filter are characterized by the parameter $m = 24.26\ \Omega/14.75\ \Omega = 1.645$. Substituting the value of m in (10), we get the calculated value of $f_2/f_0 = 5.98$, which is close enough to the measured value.

The rejection band of this filter at the attenuation level 30 dB is characterized by the ratio of the boundary frequencies $f_{\max}/f_{\min} = 5.44$. For comparison, we note that the third-order BPF [23] with $\lambda/2$ and $\lambda/4$ resonators, using

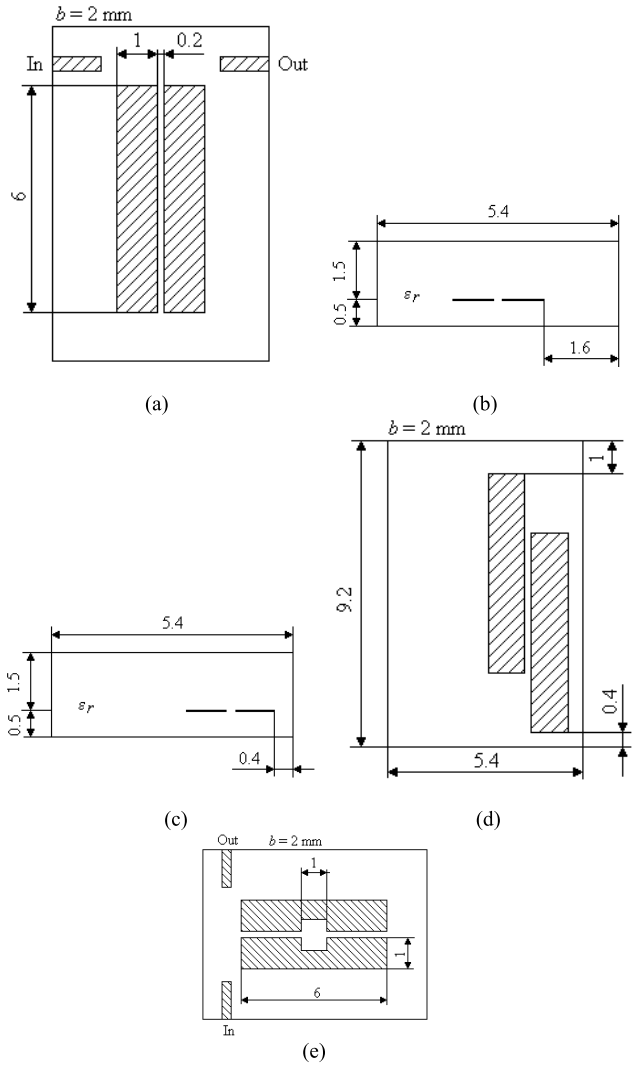

Fig. 16. Pairs of stripline half-wave resonators. (a) Symmetrical positioned. (b) Offset down. (c) Offset down and to the right. (d) Displaced downward to the right and with respect to each other. (e) SIRs of a half-wave type.

discriminating coupling K_1, has rejection band from 2.1 to 8.6 GHz ($f_{\max}/f_{\min} = 4.09$).

V. Invariance of Coupling Coefficients Relative to Dielectric Constant

Consider the influence of the dielectric constant ε_r on the coupling coefficient K between stripline resonators at the main resonant frequency f_0. To exclude the influence of a short circuit on K, we will use half-wave resonators.

A. Different Location of Stripline Half-Wave Resonators

Fig. 16(a) shows the topology of half-wave resonators, which are located in the middle of stripline construction. As in Fig. 1(a), the side surfaces of the strip structure are metallized, which makes the structure insulated. When simulating with Microwave Office (AWR), we use the following parameters: $b = 2$ mm, $L = 6$ mm, $w = 1$ mm, and $S = 0.2$ mm. Dimensions of the topological layout are 9.2 mm × 5.4 mm; center conductors are separated from metallized ends by 1.6 mm. In case $\varepsilon_r = 9.7$, we get the following values: $f_e = 7220$ MHz and $f_o = 7604$ MHz. Calculation by (1) gives the value of the coupling coefficient: $K = 0.005177$. If a permittivity $\varepsilon_r = 9.7$ is changed to $\varepsilon_r = 2.2$, then we obtain $f_e = 15159$ MHz, $f_o = 15965$ MHz, and $K = 0.05176$. Table III presents the values of K for different values of ε_r. Values of K remain almost unchanged for different values of ε_r, and only coupling frequencies f_e and f_o vary.

TABLE III
Coupling Coefficients of Stripline Resonators [Fig. 16(a)]

ε_r	2.2	9.7	21	38	92
K_{co}	0.05176	0.05177	0.05178	0.05177	0.05170

In Fig. 16(b), center conductors of resonators are shifted downward by 0.5 mm. In this case, K varies from 0.0383 to 0.0384 when ε_r varies from 2.2 to 92. In Fig. 16(c), center conductors are shifted downward and to the right, and resonance frequencies of resonators are different. Closeness of metal increases the resonance frequency of the right resonator. If the resonators are not identical, coefficient K is calculated from a more general expression as follows [8]:

$$K = \pm\frac{1}{2}\left(\frac{f_2}{f_1} + \frac{f_1}{f_2}\right)\sqrt{\left(\frac{f_o^2 - f_e^2}{f_o^2 + f_e^2}\right)^2 - \left(\frac{f_2^2 - f_1^2}{f_2^2 + f_1^2}\right)^2}. \quad (11)$$

In (11), f_1 and f_2 are the resonance frequencies of the first and second resonators. For the pair of resonators shown in Fig. 16(c), $K = 0.0352$–0.0355 when ε_r varies from 2.2 to 92. The most general case of arrangement of stripline resonators is shown in Fig. 16(d), when center conductors are shifted additionally relative to each other. This pair of resonators has $K = 0.1053$–0.1055 when ε_r varies from 2.2 to 92.

The topology of SIRs of half-wave type is shown in Fig. 16(d). Rectangles with dimensions of 1 mm × 0.4 mm are removed in the center part of strips with dimensions of 6 mm × 1 mm. In this case, the coupling coefficient is mixed and negative. When ε_r changes from 2.2 to 92, the value of K changes from -0.0613 to -0.0614.

The results of the computer simulation considered above led to the following conclusion. The EM coupling coefficient of resonators in a stripline structure with homogeneous dielectric filling and metallized lateral surfaces depends only on geometric parameters of the structure and is independent of the value of dielectric constant ε_r.

B. Dependence of Coupling Coefficient on Resonators' Length

The influence of geometric parameters, permittivity ε_r, and operating frequency f_0 on the value of coupling coefficient K in stripline resonators was analyzed in Section II. The regularity revealed above leads to the necessity of reconsideration of the influence of last two factors on K.

Let us consider the influence of resonator's length on K in more detail. We return to the pair of half-wave stripline resonators [Fig. 16(a)]. Since the permittivity does not affect

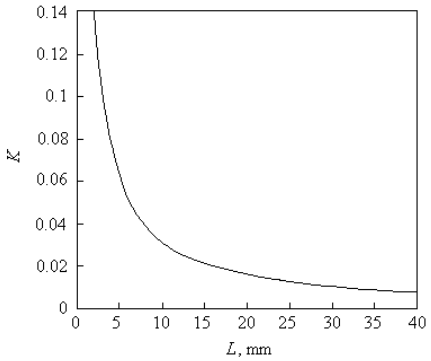

Fig. 17. Dependence of coupling coefficient on length of stripline half-wave resonators with parameters $b = 2$ mm, $w = 1$ mm, $S = 0.2$ mm.

the value of coefficient K, we can use any value of ε_r in simulation. As before, let us specify remaining parameters of the pair of resonators: $b = 2$ mm, $w = 1$ mm, and $S = 0.2$ mm. The dependence of coupling coefficient K on length L of half-wave stripline resonators is presented in Fig. 17. This dependence is evidence of the strong influence of length L on the coupling coefficient: the smaller the L is, the larger is the K.

It should be noted that quarter-wave resonators have the same coupling coefficients as half-wave resonators, but their length is only half as large. The dependence $K = K(L)$ (Fig. 17) is of practical importance. It is applicable to stripline structures with a great number of permittivity ε_r values, therefore, it is universal.

Let us return to the dependencies in Fig. 2. It seems that an increase in ε_r and operating frequency leads to an increase in K. Actually, the increase in K of stripline resonators associated with an increase in ε_r at a fixed frequency and with an increase in the operating frequency is caused by a decrease in the resonator length.

The value of K of stripline resonators can also be increased by increasing the stripline thickness b, decreasing the width w of resonator conductor, and decreasing the gap S between them. These quantities are geometric parameters of the stripline structure.

C. Stripline BPF With Different ε_r

The role of the dielectric constant ε_r is to move coupling frequencies of a stripline without changing the ratio between these frequencies. Let us consider a thin ($b = 1$ mm) fourth-order stripline filter with homogeneous dielectric weakly coupled with input and output loads [Fig. 18(a)]. The filter contains half-wave SIRs. The resonators are characterized by the following parameters: $L = 4.4$ mm and $w = 1.1$ mm. The rectangles with dimensions of 0.9 mm $\times$ 0.4 mm are removed in their center parts. The gap between resonators 2–3 is 0.25 mm, and the gap between resonators 1–2 and 3–4 is 0.3 mm. The filter dimensions are 7.05 mm $\times$ 5.9 mm $\times$ 1 mm. The coupling coefficients of the filter are mixed and have positive and negative signs.

If the end resonators are weakly coupled with loads, coupling frequencies are clearly seen in the filter's insertion loss function. We denote these frequencies by f_1, f_2, f_3, and f_4. The coupling frequencies of the filter with dielectric constant $\varepsilon_r = 92$ are shown in Fig. 18(b): $f_1 = 2923$ MHz, $f_2 = 2982$ MHz, $f_3 = 3068$ MHz, and $f_4 = 3105$ MHz. If permittivity ε_r is decreased by a factor of four and is assumed to be 23, all coupling frequencies increase exactly by a factor of two: $f_1 = 5846$ MHz, $f_2 = 5964$ MHz, $f_3 = 6136$ MHz, and $f_4 = 6210$ MHz [Fig. 18(c)]. The relation between coupling frequencies in a high-order stripline BPF with homogeneous dielectric and metallized lateral surfaces depends only on geometric parameters and it is independent of the ε_r value.

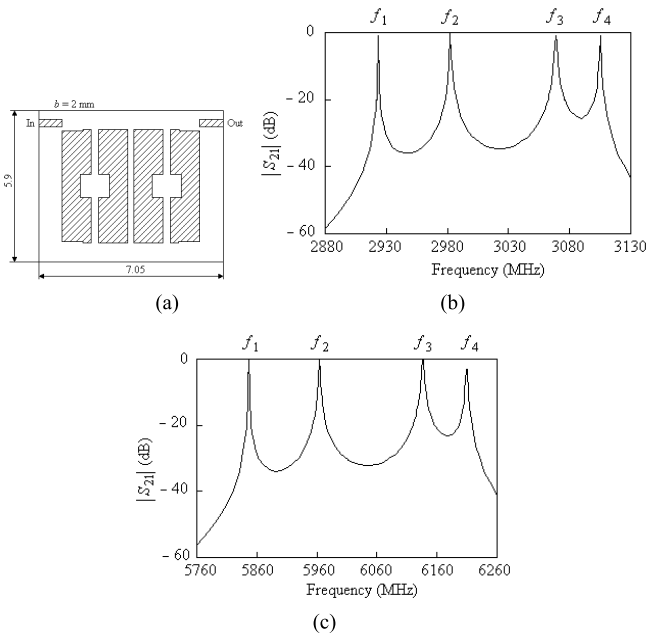

Fig. 18. Stripline fourth-order BPF. (a) Topology. (b) Coupling frequencies for $\varepsilon_r = 92$. (c) Coupling frequencies for $\varepsilon_r = 23$.

This regularity allows us to repeat frequency characteristics of the same filter design in different frequency ranges by changing the value of ε_r. The presented statements highlight that lateral surfaces of the stripline structure should be metallized. In other words, these structures should be insulated EM structures. Extremely small coupling of end resonators with loads serves as an approximation to such systems. The value of dielectric constant ε_r does not affect the relation between the coupling frequencies only in the case of complete insulation. When passing to the filter characteristics, it is necessary to increase coupling of the end resonators with loads, the EM system ceases to be insulated, and frequencies of the end resonated are detuned. The following question arises: what is required for keeping the filter frequency response under variations in ε_r?

Coupling of the end resonators with the load is characterized by external Q factor Q_e. The lesser the Q_e, the more this coupling is. Let us consider the most widespread method for connection of the load to the half-wave resonator via a short conductive section. If we neglect the length of this section, the value of Q_e can be calculated from the expression as follows:

$$Q_e = \frac{\pi R_L}{2Z_0 \sin^2 \theta'}, \quad \theta' \le \pi/2 \tag{12}$$

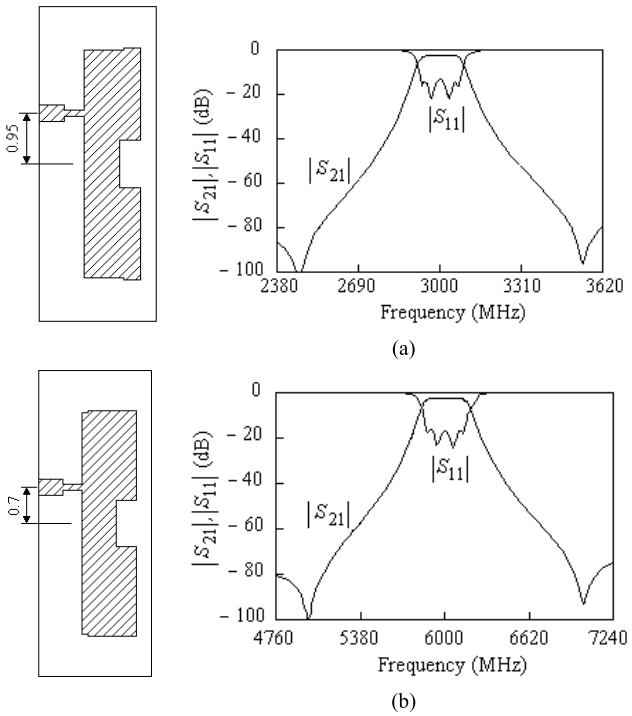

Fig. 19. Connecting loads and simulated frequency responses of stripline BPF shown at Fig. 18. (a) For case $\varepsilon_r = 92$, $f_0 = 3000$ MHz and BW = 140 MHz. (b) For case $\varepsilon_r = 23$, $f_0 = 6000$ MHz and BW = 280 MHz.

where $R_L = 50\ \Omega$ is the load resistance, and θ' is the load connection coordinate counted from the middle of the resonator. If we reduce the dielectric constant ε_r, then the value of Z_0 will increase, and Q_e (12) will decrease. In order to keep the former value of Q_e, it is necessary to decrease θ'.

The considered filter [Fig. 18(a)] contains SIRs, for which expression (12) is not legitimate. However, the pattern of variation in the load connection coordinate associated with the changing of the ε_r value is retained. Two variants of load connection and frequency responses of the filter, which correspond to values of $\varepsilon_r = 92$ and 23, are shown in Fig. 19. It is important to note that, simultaneously with shifting the load connection point toward the middle point of the resonator, it is necessary to elongate the resonator itself. This neutralizes the frequency drift associated with variation in the load connection coordinate.

After changes of ε_r by a factor of four from 92 to 23, the normalized frequency characteristics remained the same. The center frequency was doubled from 3000 to 6000 MHz. The absolute bandwidth also changed by a factor of two from 140 to 280 MHz. In general, these changes occur at $(\varepsilon_{r2}/\varepsilon_{r1})^{1/2}$ times.

Thus, if the completed design of a stripline BPF has good frequency response, it can be reproduced in another frequency band by means of appropriate selection of ε_r and minor changes in the end resonators. This pattern also applies to a stripline BPF with quarter-wave resonators and to coupling coefficients at higher resonant frequencies. Fig. 20 shows the simulated and measured frequency responses of low-profile BPF (Fig. 13), whose dielectric constant ε_r was changed

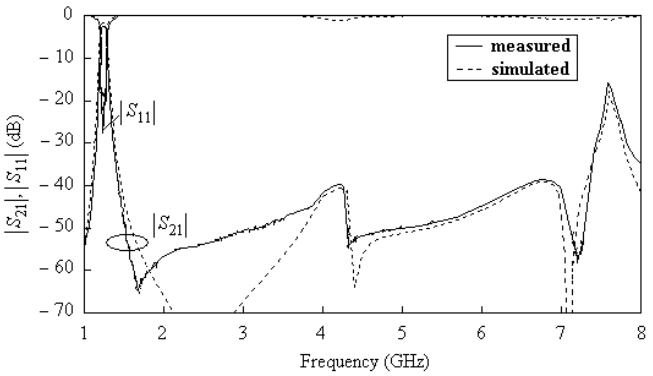

Fig. 20. Frequency responses of the modified low-profile stripline BPF shown in Fig. 13.

from 9.7 to 38, the end resonators are somewhat shortened, and the coordinate of the connection of loads t is increased from 1.2 to 1.8 mm.

In this case, we have $(\varepsilon_{r2}/\varepsilon_{r1})^{1/2} \approx 1.98$. The value of f_0 decreased by the same amount from 2450 to 1240 MHz, and BW changed from 140 to 71 MHz. It is important to note that the "zero" value of the coupling coefficient at the frequency of the first spurious resonance $K_1 \approx 0$ is preserved and we get a BPF with a wide rejection band in this case as well.

VI. Conclusion

The studied patterns of coupling coefficients in combline and pseudocombline stripline BPFs allow us to realize a significant variety of frequency responses. It has been found that there is EM coupling between the stripline combline ($\lambda/4$) resonators, and the stripline combline structure is BPF. Mixed coupling coefficients between SIRs and the simultaneous use of substrates with high dielectric constant allow us to implement the quasi-elliptic small-sized stripline BPFs with high selectivity. Zero coupling coefficient ($K_1 = 0$) at the first spurious resonant frequency of SIRs [Fig.11(c)] and thin substrates ($h \leq 0.5$ mm) allows us to create thin ($b \leq 1$ mm) stripline BPFs with extended rejection band. The established property of the invariance of the coupling coefficients with respect to ε_r in isolated stripline structures allows us to move the same frequency response on the frequency axis by changing ε_r only. Stripline BPFs have great potential.

References

[1] G. L. Matthaei, L. Young, and E. M. T. Jones, *Microwave Filters, Impedance-Matching Network, and Coupling Structures*. Norwood, MA, USA: Artech House, 1980.

[2] M. Makimoto and S. Yamashita, *Microwave Resonators and Filters for Wireless Communication. Theory, Design and Application*. Berlin, Germany: Springer-Verlag, 2001.

[3] A. Fukasawa, "Analysis and composition of a new microwave filter configuration with inhomogeneous dielectric medium," *IEEE Trans. Microw. Theory Techn.*, vol. MTT-30, no. 9, pp. 1367–1375, Sep. 1982.

[4] D. Morgan, *Surface Acoustic Wave Filters: With Applications to Electronic Communications and Signal Processing*. New York, NY, USA: Academic, 2010.

[5] L. K. Yeung, K.-L. Wu, and Y. E. Wang, "Low-temperature cofired ceramic LC filters for RF applications [applications notes]," *IEEE Microw. Mag.*, vol. 9, no. 5, pp. 118–128, Oct. 2008.

[6] T. Ishizaki, M. Fujita, H. Kagata, T. Uwano, and H. Miyake, "A very small dielectric planar filter for portable telephones," *IEEE Trans. Microw. Theory Techn.*, vol. 42, no. 11, pp. 2017–2022, Nov. 1994.
[7] J. Bolljahn and G. Matthaei, "A study of the phase and filter properties of arrays of parallel conductors between ground planes," *Proc. IRE*, vol. 50, no. 3, pp. 299–311, Mar. 1962.
[8] J.-S. Hong, *Microstrip Filters for RF/Microwave Application*, 2nd ed. New York, NY, USA: Wiley, 2011.
[9] L. N. Dworsky, "Stripline filters," in *Proc. IEEE 37th Annu. Freq. Control Symp.*, Philadelphia, PA USA, Jun. 1983, pp. 387–393.
[10] L. Szydlowski, A. Lamecki, and M. Mrozowski, "Coupled-resonator filters with frequency-dependent couplings: Coupling matrix synthesis," *IEEE Microw. Wireless Compon. Lett.*, vol. 22, no. 6, pp. 312–314, Jun. 2012.
[11] R. Levy, "New cascaded trisections with resonant cross-couplings (CTR sections) applied to the design of optimal filters," in *IEEE MTT-S Int. Microw. Symp. Dig.*, vol. 2, Jun. 2004, pp. 447–450.
[12] H. Wang and Q.-X. Chu, "An inline coaxial quasi-elliptic filter with controllable mixed electric and magnetic coupling," *IEEE Trans. Microw. Theory Techn.*, vol. 57, no. 3, pp. 667–673, Mar. 2009.
[13] M. Hoft and T. Shimamura, "Design of symmetric trisection filters for compact low-temperature co-fired ceramic realization," *IEEE Trans. Microw. Theory Techn.*, vol. 58, no. 1, pp. 165–175, Jan. 2010.
[14] W. Shen, L.-S. Wu, X.-W. Sun, W.-Y. Yin, and J.-F. Mao, "Novel substrate integrated waveguide filters with mixed cross coupling (MCC)," *IEEE Microw. Wireless Compon. Lett.*, vol. 19, no. 11, pp. 701–703, Nov. 2009.
[15] K. Gong, W. Hong, Y. Zhang, P. Chen, and C. J. You, "Substrate integrated waveguide quasi-elliptic filters with controllable electric and magnetic mixed coupling," *IEEE Trans. Microw. Theory Techn.*, vol. 60, no. 10, pp. 3071–3078, Oct. 2012.
[16] L. Szydlowski, A. Jedrzejewski, and M. Mrozowski, "A trisection filter design with negative slope of frequency-dependent crosscoupling implemented in substrate integrated waveguide (SIW)," *IEEE Microw. Wireless Compon. Lett.*, vol. 23, no. 9, pp. 456–458, Sep. 2013.
[17] K. Ma, J.-G. Ma, K. S. Yeo, and M. A. Do, "A compact size coupling controllable filter with separate electric and magnetic coupling paths," *IEEE Trans. Microw. Theory Techn.*, vol. 54, no. 3, pp. 1113–1119, Mar. 2006.
[18] Q.-X. Chu and H. Wang, "A compact open-loop filter with mixed electric and magnetic coupling," *IEEE Trans. Microw. Theory Techn.*, vol. 56, no. 2, pp. 431–439, Feb. 2008.
[19] F. Zhu, W. Hong, J.-X. Chen, and K. Wu, "Quarter-wavelength stepped-impedance resonator filter with mixed electric and magnetic coupling," *IEEE Microw. Wireless Compon. Lett.*, vol. 24, no. 2, pp. 90–92, Feb. 2014.
[20] A. Zakharov, S. Rozenko, and M. Ilchenko, "Two types of trisection bandpass filters with mixed cross-coupling," *IEEE Microw. Wireless Compon. Lett.*, vol. 28, no. 7, pp. 585–587, Jul. 2018.
[21] A. Zakharov and M. Ilchenko, "Trisection microstrip delay line filter with mixed cross-coupling," *IEEE Microw. Wireless Compon. Lett.*, vol. 27, no. 12, pp. 1083–1085, Dec. 2017.
[22] X. Yin Zhang and Q. Xue, "Harmonic-suppressed bandpass filter based on discriminating coupling," *IEEE Microw. Wireless Compon. Lett.*, vol. 19, no. 11, pp. 695–697, Nov. 2009.
[23] Y. C. Li, X. Y. Zhang, and Q. Xue, "Bandpass filter using discriminating coupling for extended out-of-band suppression," *IEEE Microw. Wireless Compon. Lett.*, vol. 20, no. 7, pp. 369–371, Jul. 2010.
[24] S.-C. Lin, Y.-S. Lin, and C.-H. Chen, "Extended-stopband bandpass filter using both half- and quarter-wavelength resonators," *IEEE Microw. Wireless Compon. Lett.*, vol. 16, no. 1, pp. 43–45, Jan. 2006.
[25] *High-Perf Ceramic Monoblock Filter CER0206A Data Sheet*, CTS Electron. Compon., Bloomingdale, IL, USA 2005. [Online]. Available: https://www.ctscorp.com

Alexander Zakharov received the M.S. degree in physics from Kyiv State University, Kyiv, Ukraine, in 1971, the Ph.D. degree in radio engineering from the National Technical University of Ukraine "Igor Sikorsky Kyiv Polytechnic Institute," Kyiv, in 1986, and the D.Sc. degree in solid state electronics from the Cybernetics Institute of Academy of Science, Kyiv, in 1994.

From 1971 to 1988, he was a Lecturer with the Kyiv Aviation College, Kyiv. In 1988, he joined as a Researcher with the Telecommunication Department, National Technical University of Ukraine "Igor Sikorsky Kyiv Polytechnic Institute," where he is currently the Head Scientist. His current research interests include, RF/microwave filters and duplexers for telecommunication systems, circuits theory, and nonuniform transmission line resonators.

Michael Ilchenko (Senior Member, IEEE) received the M.S. and Ph.D. degrees in radio engineering from the National Technical University of Ukraine "Igor Sikorsky Kyiv Polytechnic Institute," Kyiv, Ukraine, in 1964 and 1967, respectively, and the D.Sc. degree in solid state electronics from the Cybernetics Institute, National Academy of Sciences at Ukraine (NASU), Kyiv, in 1980.

He was a Senior Researcher and an Assistant Professor with the National Technical University of Ukraine "Igor Sikorsky Kyiv Polytechnic Institute," where he has been a Full Professor since 1982 and has been Pro-Rector for Research since 1988. He is currently the Director of the Telecommunication Department, National Technical University of Ukraine "Igor Sikorsky Kyiv Polytechnic Institute." He has authored or coauthored several books, and one of the books, namely *Dielectric Resonators* in 1989, is available with the US Library of Congress. Since 1997, he has been an Active Member (Academician) with NASU. His current interest includes microwave technologies in telecommunications systems.

Dr. Ilchenko was a recipient of three Ukrainian State Prizes and three awards for Science and Technology Excellence.